Order by Quenched Disorder in the Model Triangular Antiferromagnet RbFe(MoO₄)₂

A. I. Smirnov, ¹ T. A. Soldatov, ^{1,2} O. A. Petrenko, ³ A. Takata, ⁴ T. Kida, ⁴ M. Hagiwara, ⁴
A. Ya. Shapiro, ⁵ and M. E. Zhitomirsky ⁶

¹P. L. Kapitza Institute for Physical Problems, RAS, 119334 Moscow, Russia

²Moscow Institute for Physics and Technology, 141700 Dolgoprudny, Russia

³Department of Physics, University of Warwick, Coventry CV4 7AL, United Kingdom

⁴Center for Advanced High Magnetic Field Science (AHMF), Osaka University, Osaka 560-0043, Japan

⁵A. V. Shubnikov Institute for Crystallography RAS, 119333 Moscow, Russia

⁶CEA, INAC-PHELIQS, F-38000 Grenoble, France

(Received 29 March 2017; published 26 July 2017)

We observe a disappearance of the 1/3 magnetization plateau and a striking change of the magnetic configuration under a moderate doping of the model triangular antiferromagnet RbFe(MoO₄)₂. The reason is an effective lifting of degeneracy of mean-field ground states by a random potential of impurities, which compensates, in the low-temperature limit, the fluctuation contribution to free energy. These results provide a direct experimental confirmation of the fluctuation origin of the ground state in a real frustrated system. The change of the ground state to a least collinear configuration reveals an effective positive biquadratic exchange provided by the structural disorder. On heating, doped samples regain the structure of a pure compound, thus allowing for an investigation of the remarkable competition between thermal and structural disorder.

DOI: 10.1103/PhysRevLett.119.047204

Triangular-lattice antiferromagnets (TLAFs) form a popular class of magnetic materials that provides paradigmatic cases of magnetic frustration [1] and intrinsic multiferroicity [2,3]. A spectacular manifestation of frustration in TLAFs is the 1/3 magnetization plateau with the up-updown (uud) spin structure stabilized by fluctuations out of a degenerate manifold of classical ground states [4–6]. A 1/3 magnetization plateau has been experimentally observed in a number of TLAFs [7–11]. Generally, it is a challenging task to distinguish the pure frustration-driven plateaus from those produced by additional perturbations, such as an Ising anisotropy or magnetoelastic coupling. The latter mechanism is responsible for the 1/2 magnetization plateau in chromium spinels [12–14], whereas an Ising anisotropy may contribute to the 1/3 plateau in some triangular antiferromagnets [9,10]. Thus, a direct verification of the plateau mechanism remains a pressing issue in the field of frustrated magnetism.

An experimental test to determine if fluctuations are at the origin of the magnetization plateau states in TLAFs has recently been suggested [15]. It was shown theoretically that the frustration-driven plateaus become unstable in the presence of a weak structural disorder either in the form of nonmagnetic dilution or as an exchange-bond randomness. Weak disorder in frustrated magnets makes an energetic selection among degenerate ground states that competes with the effect of thermal or quantum fluctuations. Besides the plateau smearing, in fields below the plateau, the structural disorder may also stabilize umbrella- or fan-type magnetic structures instead of the more collinear states selected by fluctuations in clean TLAFs [4–6]. The strong

influence of a weak doping is due to a high degree of degeneracy in a magnet with a fluctuation-selected ground state and will not give a comparable effect in systems with a pronounced minimum of the mean-field energy. Thus, the experimental observation of the plateau vanishing and of a ground state changing on doping serves as direct evidence of the fluctuation origin of corresponding phases in pure crystals with magnetic frustration. At the phenomenological level, the effect of structural disorder on degeneracy lifting in frustrated magnets may be represented by an effective biquadratic exchange with a positive sign [15–19]. In a different context, a positive biquadratic exchange was shown to be generated by surface roughness in ferromagnetic multilayers [20], where it leads to the experimentally observed 90° orientation of magnetizations [21,22].

Our work is motivated by a search for direct experimental evidence for a disorder-induced positive biquadratic exchange in bulk frustrated magnets. We also seek to verify experimentally the fluctuation nature of the ground state of a pure TLAF and to observe the competition between static and dynamic disorder. The material chosen for the study is RbFe(MoO₄)₂, a magnetic compound featuring triangular-lattice layers of Fe³⁺ ions with semiclassical S = 5/2 spins. The system has an easy-plane magnetic anisotropy with the plane parallel to layers and exhibits a 1/3 magnetization plateau only for $H \perp c$ (the caxis is normal to the Fe³⁺ layers) [23,24]. Random exchange-bond modulations in triangular layers is achieved by substituting K for Rb in the interlayer space. In this Letter, we present experimental results that demonstrate a rapid disappearance of the plateau on K doping, whereas the Néel temperature T_N , the saturation field $H_{\rm sat}$, and the antiferromagnetic resonance gap Δ are all changed by less than 15%. Furthermore, the electron spin resonance (ESR) measurements also reveal a drastic change of the spin structure with doping at fields below the plateau.

The crystals of $Rb_{1-x}K_xFe(MoO_4)_2$ were prepared as previously described [8]. In addition to a controlled amount of K, about 1 atomic percent of Al was also found in some samples. This aluminum impurity probably comes from the corundum crucible and is a likely reason for the observed dispersion in T_N of about ± 0.2 K for the samples with the same x. In the limiting case of KFe(MoO₄)₂ (x = 1), we get an ~50% reduction of the principal exchange constant [25]. The magnetization curves M(H) and susceptibility were studied by means of the vibrating sample magnetometer in magnetic fields up to 10 T and by a pulsed field method in the 30 T range using the 55 T magnet at the AHMF center in Osaka University. Multifrequency 25– 150 GHz ESR was used to determine the zero-field energy gap at the AHMF center and to derive frequency-field diagrams and angular dependencies of ESR absorption at the Kapitza Institute.

The magnetization plateau for the pure sample (as illustrated in the inset in Fig. 1) is clearly marked by a significant reduction in the derivative, dM/dH, measured for $\mathbf{H} \perp c$. The development of the dM(H)/dH curves on doping is presented in the left panel in Fig. 1. At T=1.4 K, the decrease in the dM/dH value on the plateau becomes smaller with doping, and for x=0.15 the plateau completely disappears. However, the temperature evolution of dM(H)/dH curves for this x=0.15

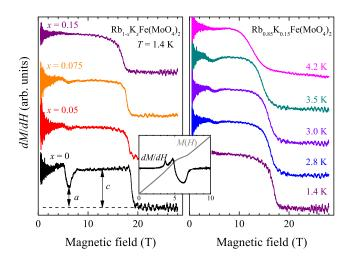


FIG. 1. (Left) dM/dH vs field curves for the Rb_{1-x}K_xFe(MoO₄)₂ crystals with different x, measured in the pulse field $\mathbf{H} \perp c$ at T=1.4 K. Parameters a and c are used to define a plateau quality factor Q (see the main text). (Inset) M(H) and dM(H)/dH curves taken for a pure sample at the same temperature in steady fields using a vibrating sample magnetometer. (Right) dM/dH vs field curves for the x=0.15 sample measured in the pulsed field $\mathbf{H} \perp c$ at different temperatures.

sample shows that the plateau is restored, at least partially, on heating. The local minimum in the derivative appears again near 6 T for T=2.8 K and remains clearly visible at 3.0 and 3.5 K, as shown in Fig. 1, right panel. We present here only the records of the dM(H)/dH curves for a decreasing magnetic field, as this sweep direction helps to avoid the sample heating caused by a magnetocaloric effect. The full collection of the dM(H)/dH curves for both increasing and decreasing fields is given in Supplemental Material [26].

We introduce a *quality* factor Q = 1 - a/c to characterize the magnetization plateau. Here a is the value of the dM/dH at its minimum on a plateau, and c is the value of the dM/dH for the fields between the plateau and magnetization saturation, as defined in Fig. 1. For an ideal, perfectly flat plateau, Q = 1, while Q = 0 corresponds to the absence of the plateau. The dependence of Q on doping and temperature (see Fig. 2) shows a disappearance of the plateau on doping and its restoration on heating. The value of H_{sat} is defined as a field where dM/dH decreases by 50% compared to its value just above a plateau. The value of $\mu_0 H_{\text{sat}}$ measured at $T=1.4\,$ K decreases on doping from 18.6 T in a pure sample to 16.7 T for x = 0.15. An empirical width of the field transition to a saturation, estimated as a field interval where the dM/dH varies between 0.75 and 0.25 of the maximum value, is 0.3 T for the x = 0 sample, and it increases to about 1.0 T for the x = 0.15 sample but is still much smaller than the saturation field itself. Using a similar criterion, that the change of derivative dM/dT varies between 0.75 and 0.25 of the maximum value, the transition width ΔT at T_N can also be estimated. ΔT is about 0.1 K for all x, except x = 0.05, where it is 0.3 K, thus showing that the transition region is significantly smaller than T_N . On doping, the value of T_N decreases from 4.1 for x = 0 to 3.0 K for the x = 0.15sample. The x dependencies of the normalized values of T_N and $H_{\rm sat}$ are presented in the left panel in Fig. 2.

The ESR spectra of a nominally pure sample (left panels in Fig. 3) have an energy gap of $\Delta_0 \simeq 90$ GHz and for $H \perp c$ consist of the two frequency branches, ascending and

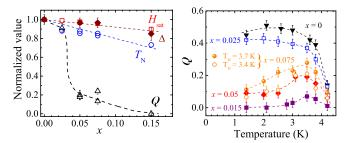


FIG. 2. (Left) Normalized values of Néel temperature T_N , saturation field $H_{\rm sat}$, excitation gap Δ , and plateau quality factor Q vs doping. (Right) Plateau quality factor Q vs temperature for samples with different doping concentrations. Dashed lines are guides to the eyes.

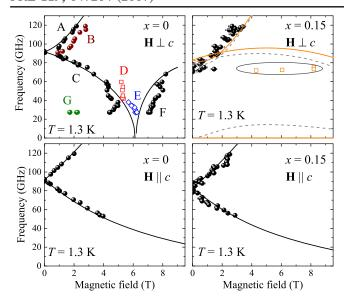


FIG. 3. Frequency-field diagrams of the $\mathrm{Rb}_{1-x}\mathrm{K}_x\mathrm{Fe}(\mathrm{MoO_4})_2$ samples for x=0 (left-hand side panels) and x=0.15 (right-hand side panels). The top and bottom panels show the ESR frequencies for $H\bot c$ and $H\|c$, respectively. The experimental results (symbols) are compared to the calculations (solid lines) for the Y/umbrella structure with $J=1.1J_0$, $D=D_0$ for x=0 and for the inverted Y (\bar{Y})/umbrella state with $J=0.9J_0$, $D=D_0$ for x=0.15; see the main text for the notations. Dashed lines represent a calculation for the \bar{Y} state with K/J=0.01, while the ellipse covers a wide area of weak absorption.

descending with an applied magnetic field in agreement with the previous results [8,24]. The ascending branch is split into two closely positioned branches (A) and (B) by the weak interplane interactions. The frequency of the descending branch (C) is reduced almost to zero for the field approaching the lower boundary of the plateau, while another mode (D), of a higher frequency, appears near the entrance of the plateau. Modes in the middle of the plateau (E) and at the upper boundary (F) are also detected in qualitative agreement with the theory [6] and previous experiments [8]. Finally, a weakly absorbing mode (G) near 30 GHz appears due to a splitting of the zero-frequency mode [8]. A full record of the microwave absorption vs magnetic field at different frequencies is given in Supplemental Material [26].

The frequency-field dependencies for the x=0.15 sample are shown in the right-hand panels in Fig. 3. The gap Δ is reduced to (75 ± 5) GHz on doping, and its evolution with doping concentration x is shown in Fig. 2. For a pure sample, ESR lines are observed both above and below Δ_0 for $\mathbf{H} \perp c$, while for the x=0.15 sample only the ascending ESR branch is detected. The descending ESR branch either disappears or transforms in a field-independent mode on doping. For the field $\mathbf{H} \parallel c$, both the ascending and descending branches are visible for pure and all doped samples; see the lower panels in Fig. 3 and Ref. [26]. The angular dependence of the ESR absorption, presented in

Ref. [26], reveals that, upon rotating from $\mathbf{H} \parallel c$ to $\mathbf{H} \perp c$, the ESR line of the descending branch is smeared at a deviation from the c axis and disappears completely for $\mathbf{H} \perp c$ in the x=0.15 sample, while it is conserved in a pure sample. This observation gives a direct confirmation of the disappearance of the descending ESR branch on doping.

To model the observed behavior of doped $RbFe(MoO_4)_2$, we use the spin Hamiltonian

$$\hat{\mathcal{H}} = \sum_{\langle ij \rangle} J_{ij} \mathbf{S}_i \cdot \mathbf{S}_j + D \sum_i (S_i^z)^2 - g\mu_B \sum_i \mathbf{H} \cdot \mathbf{S}_i. \quad (1)$$

The nearest-neighbor exchange constant J_{ij} is assumed to have a weak random variation between the bonds: $J_{ij} = \langle J_{ij} \rangle + \delta J_{ij}, \ \langle \delta J_{ij} \delta J_{kl} \rangle = \delta J^2 \delta_{ij,kl}, \$ and $\delta J \ll J = \langle J_{ij} \rangle.$ Inelastic neutron scattering experiments yield $J_0 = 0.086$ meV and $D_0 = 0.027$ meV for RbFe(MoO₄)₂ [27]. The effect of bond disorder and/or thermal and quantum fluctuations can be semiquantitatively represented by adding a biquadratic term

$$\hat{\mathcal{H}}_B = K \sum_{\langle ij \rangle} (\mathbf{S}_i \cdot \mathbf{S}_j)^2. \tag{2}$$

For the purely Heisenberg model (1) with D=0, $\delta J_{ij}=0$, the quantum fluctuations contribute $K_Q \simeq -J/(24S^3)$ [28]. A negative sign for the biquadratic constant K means that fluctuations select the most collinear or coplanar states, resulting in a standard sequence of the ordered states as the field increases; see Figs. 4(a)–4(c) [6]. A frozen bond disorder instead generates a positive biquadratic contribution, $K_{\rm dis}=\delta J^2/(3JS^2)$ [15]. For $(\delta J/J)^2>1/(8S)$, the disorder effect becomes dominant, and the stable magnetic states are found by minimizing a Hamiltonian, which combines (1) and (2) with K>0. One can straightforwardly verify that in such a case the least collinear states are energetically preferred. For the planar spin system (D>0),

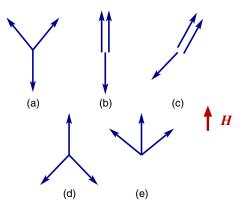


FIG. 4. Spin structures appearing for the pure TLAF in an applied field: (a) the Y state, (b) the uud state, and (c) the 2:1 state. Spin structures of a planar triangular antiferromagnet in the presence of structural disorder: (d) the \bar{Y} state and (e) the fan state.

this is the inverted $Y(\bar{Y})$ state [Fig. 4(d)], which continuously transforms into the fan state in higher fields [Fig. 4(e)]. Small variations in the direction of the local anisotropy axis may also contribute to a lifting of the degeneracy and $K_{\rm dis}$, but this weak effect is ignored as D < J.

The two possible low-field magnetic structures, the Y and the \bar{Y} states, have qualitatively different ESR spectra for in-plane orientations of an applied field. This fact fully agrees with the idea of an order-by-disorder effect, which relates the lifting of degeneracy in frustrated magnets to the excitation spectra of the different ground states [29,30]. Performing the standard spin-wave calculations for (1), we obtain two resonance frequencies:

$$\omega_1 = 3JS\sqrt{d(1 \mp h)(3 \pm h)}, \qquad d = \frac{D}{3J}$$

$$\omega_2 = 3JS\sqrt{2d + h^2 + d(1 \pm h)^2}, \qquad h = \frac{g\mu_B H}{3JS}, \qquad (3)$$

where the upper (lower) sign corresponds to the Y (\bar{Y}) state. The third ESR branch vanishes in the harmonic approximation $\omega_3=0$ reflecting the remaining classical degeneracy.

For $H \perp c$, the ESR frequencies of pure RbFe(MoO₄)₂, shown in the upper left panel in Fig. 3, are accurately described by the expressions (3) for the Y state with J = $1.1J_0$ and $D=D_0$, the values that are marginally different from the ones obtained in the neutron scattering experiments [27]. The agreement between the theory and experiment is good despite the presence of the incommensurate spiral state in low fields [3], which may indicate significant Y-type distortions of the spiral structure induced by an external field. The same microscopic parameters also nicely fit the ESR data for H||c| (the lower left panel in Fig. 3); see also [26]. The characteristic feature of the ESR spectra for the Y state $(H \perp c)$ is the descending branch $\omega_1(H)$ that corresponds to the out-of plane oscillations of the two spin sublattices about the field direction, while the third sublattice remains parallel to the field. The frequency of this mode decreases to zero upon a transition into the collinear *uud* structure at $\mu_0 H \approx 6$ T. In contrast, the frequency of the same mode for the \bar{Y} state, which remains noncollinear, exhibits little variation in the corresponding field region. Thus, the absence of the descending ESR branch for the doped samples for $H \perp c$ clearly indicates a change of the spin structure. We compare the ESR data for the x = 0.15doped sample with the theoretical frequencies (3) for the \bar{Y} state on the upper right panel in Fig. 3. A somewhat smaller averaged value of $J = 0.9J_0$ ($D = D_0$) used for the fit is consistent with a local reduction of the exchange interaction induced by K impurities.

The biquadratic interaction (2) has been derived as an effective potential in the manifold of degenerate classical ground states [28]. Nevertheless, the effect of structural

disorder on the q=0 excitations in the \bar{Y} state beyond substituting averaged J and D can be estimated by explicitly including $\hat{\mathcal{H}}_B$ in the calculations. One should bear in mind that an effective biquadratic interaction is rather weak. Using $K_{\rm dis}=\delta J^2/(3JS^2)$ [15] and noting that the local $\delta J/J\simeq 50\%$, we find that the biquadratic constant does not exceed $K_{\rm dis}/J=0.01$ –0.02, whereas $K_Q/J\simeq -3\times 10^{-3}$. We show in the upper right panel in Fig. 3 the ESR modes computed for $J=0.9J_0$, $D=D_0$, and K/J=0.01. The main qualitative effect of $\hat{\mathcal{H}}_B$ is a nonzero value for ω_3 , which reflects a lack of degeneracy, whereas the shift of the two upper modes is indeed tiny. The resonance frequencies for the third branch are too small to be detected in the ESR spectrometers used here.

One can see in Fig. 2 that the plateau quality Q changes drastically with doping, whereas T_N , H_{sat} , and Δ exhibit a weak linear dependence on x. The samples with the plateau suppressed or canceled by the impurities still demonstrate a sharp Néel transition, shifted down in temperature from T_N in a pure sample. The behavior of T_N , $H_{\rm sat}$, and Δ shows that the exchange interaction is not strongly affected on doping. A sharp Néel transition and a steplike change in dM/dH at saturation confirm the absence of the macroscopic inhomogeneities in the samples studied. Thus, the observed disappearance of the plateau and the change of the ground state in low fields should be ascribed only to the influence of a random potential. This statement is confirmed by the observed partial restoration of a plateau in doped samples on heating (see Fig. 2). Indeed, according to Ref. [[15]], the region of the uud phase (1/3-plateau phase) in the T-H phase diagram is shifted to a higher temperatures on doping.

In conclusion, the observed doping-induced changes of the magnetization curves and the magnetic resonance spectra of RbFe(MoO_4)₂ reveal a transition from a collinear up-up-down structure, stabilized by fluctuations, to a fan structure supported by a weak static disorder, as well as a transformation of the lower-field spin structure from the Y type to an inverted Y structure. Our experiments establish the fluctuation origin of the 1/3-plateau and the Y-type phases and show that the ground state selection process is affected by a strong competition between structural disorder and thermal fluctuations. The structural disorder is found to lead to a positive biquadratic exchange. We observe a fundamentally different behavior between pure and lightly doped samples on heating, which results in the restoration of the magnetization plateau in the doped materials, while in a pure crystal the plateau is removed. These observations provide convincing confirmation of the competition between thermal and quenched disorder, demonstrating that the negative biquadratic term arising from thermal fluctuations once again dominates at a higher temperature. Disorder-induced modifications of the magnetic structure may also be used to control multiferroicity of TLAFs and, perhaps, of other spiral antiferromagnets.

We thank S. S. Sosin and L. E. Svistov for numerous discussions. Work at the Kapitza Institute is supported by Russian Foundation for Basic Research, Grant No. 15-02-05918, by the Programs of the Presidium of Russian Academy of Sciences, high-frequency ESR measurements were supported by Russian Science Foundation Grant No. 17-02-01505. A. I. S. is indebted to Osaka University for invitation as a visiting Professor. Work at Osaka University is supported by the International Joint Research Promotion Program.

- [1] M. F. Collins and O. A. Petrenko, Can. J. Phys. 75, 605 (1997).
- [2] H. J. Lewtas, A. T. Boothroyd, M. Rotter, D. Prabhakaran, H. Müller, M. D. Le, B. Roessli, J. Gavilano, and P. Bourges, Phys. Rev. B 82, 184420 (2010).
- [3] M. Kenzelmann, G. Lawes, A. B. Harris, G. Gasparovic, C. Broholm, A. P. Ramirez, G. A. Jorge, M. Jaime, S. Park, Q. Huang, A. Ya. Shapiro, and L. A. Demianets, Phys. Rev. Lett. 98, 267205 (2007).
- [4] D. H. Lee, J. D. Joannopoulos, J. W. Negele, and D. P. Landau, Phys. Rev. Lett. **52**, 433 (1984).
- [5] H. Kawamura and S. Miyashita, J. Phys. Soc. Jpn. 54, 4530 (1985).
- [6] A. V. Chubukov and D. I. Golosov, J. Phys. Condens. Matter 3, 69 (1991).
- [7] T. Inami, Y. Ajiro, and T. Goto, J. Phys. Soc. Jpn. 65, 2374 (1996).
- [8] L. E. Svistov, A. I. Smirnov, L. A. Prozorova, O. A. Petrenko, L. N. Demianets, and A. Ya. Shapiro, Phys. Rev. B 67, 094434 (2003).
- [9] H. Kitazawa, H. Suzuki, H. Abe, J. Tang, and G. Kido, Physica (Amsterdam) 259–261B, 890 (1999).
- [10] R. Ishii, S. Tanaka, K. Onuma, Y. Nambu, M. Tokunaga, T. Sakakibara, N. Kawashima, Y. Maeno, C. Broholm, D. P. Gautreaux, J. Y. Chan, and S. Nakatsuji, Europhys. Lett. 94, 17001 (2011).
- [11] Yu. Shirata, H. Tanaka, A. Matsuo, and K. Kindo, Phys. Rev. Lett. 108, 057205 (2012).

- [12] H. Ueda, H. A. Katori, H. Mitamura, T. Goto, and H. Takagi, Phys. Rev. Lett. 94, 047202 (2005).
- [13] K. Penc, N. Shannon, and H. Shiba, Phys. Rev. Lett. 93, 197203 (2004).
- [14] H. Ueda, H. Mitamura, T. Goto, and Y. Ueda, Phys. Rev. B 73, 094415 (2006).
- [15] V. S. Maryasin and M. E. Zhitomirsky, Phys. Rev. Lett. 111, 247201 (2013).
- [16] C. L. Henley, Phys. Rev. Lett. 62, 2056 (1989).
- [17] M. W. Long, J. Phys. Condens. Matter 1, 2857 (1989).
- [18] Y. V. Fyodorov and E. F. Shender, J. Phys. Condens. Matter 3, 9123 (1991).
- [19] V. S. Maryasin and M. E. Zhitomirsky, J. Phys. Conf. Ser. 592, 012112 (2015).
- [20] J. C. Slonczewski, Phys. Rev. Lett. 67, 3172 (1991).
- [21] S. O. Demokritov, J. Phys. D 31, 925 (1998).
- [22] C. M. Schmidt, D. E. Bürgler, D. M. Schaller, F. Meisinger, and H.-J. Güntherodt, Phys. Rev. B 60, 4158 (1999).
- [23] L. E. Svistov, A. I. Smirnov, L. A. Prozorova, O. A. Petrenko, A. Micheler, N. Büttgen, A. Ya. Shapiro, and L. N. Demianets, Phys. Rev. B 74, 024412 (2006).
- [24] A. I. Smirnov, H. Yashiro, S. Kimura, M. Hagiwara, Y. Narumi, K. Kindo, A. Kikkawa, K. Katsumata, A. Ya. Shapiro, and L. N. Demianets, Phys. Rev. B 75, 134412 (2007).
- [25] A. I. Smirnov, L. E. Svistov, L. A. Prozorova, A. Zheludev, M. D. Lumsden, E. Ressouche, O. A. Petrenko, K. Nishikawa, S. Kimura, M. Hagiwara, K. Kindo, A. Ya. Shapiro, and L. N. Demianets, Phys. Rev. Lett. 102, 037202 (2009).
- [26] See Supplemental Material at http://link.aps.org/supplemental/10.1103/PhysRevLett.119.047204 for further experimental and theoretical details.
- [27] J. S. White, Ch. Niedermayer, G. Gasparovic, C. Broholm, J. M. S. Park, A. Ya. Shapiro, L. A. Demianets, and M. Kenzelmann, Phys. Rev. B 88, 060409 (2013).
- [28] M. E. Zhitomirsky, J. Phys. Conf. Ser. 592, 012110 (2015).
- [29] E. F. Shender, Zh. Eksp. Teor. Fiz. **83**, 326 (1982) [Sov. Phys. JETP **56**, 178 (1982)].
- [30] R. Moessner, Can. J. Phys. 79, 1283 (2001).